IEEE Access
Multidisciplinary | Rapid Review | Open Access Journal

Received September 9, 2020, accepted September 22, 2020, date of publication October 6, 2020, date of current version October 19, 2020.

Digital Object Identifier 10.1109/ACCESS.2020.3028911

Fast Multi-Objective Optimization of Antenna Structures by Means of Data-Driven Surrogates and Dimensionality Reduction

SLAWOMIR KOZIEL[1,2], (Senior Member, IEEE), AND ANNA PIETRENKO-DABROWSKA[2], (Senior Member, IEEE)
[1]Engineering Optimization and Modeling Center, Department of Technology, Reykjavik University, 101 Reykjavik, Iceland
[2]Faculty of Electronics, Telecommunications and Informatics, Gdansk University of Technology, 80-233 Gdansk, Poland

Corresponding author: Anna Pietrenko-Dabrowska (anna.dabrowska@pg.edu.pl)

This work was supported in part by the Icelandic Centre for Research (RANNIS) under Grant 206606051, and in part by the National Science Centre of Poland under Grant 2018/31/B/ST7/02369.

ABSTRACT Design of contemporary antenna structures needs to account for several and often conflicting objectives. These are pertinent to both electrical and field properties of the antenna but also its geometry (e.g., footprint minimization). For practical reasons, especially to facilitate efficient optimization, single-objective formulations are most often employed, through either a priori preference articulation, objective aggregation, or casting all but one (primary) objective into constraints. Notwithstanding, the knowledge of the best possible design trade-offs provides a more comprehensive insight into the properties of the antenna structure at hand. Genuine multi-objective optimization is a proper way of acquiring such data, typically rendered in the form of a Pareto set that represents the mentioned trade-off solutions. In antenna design, the fundamental challenge is high computational cost of multi-objective optimization, normally carried out using population-based metaheuristic algorithms. In most practical cases, the use of reliable, yet costly, full-wave electromagnetic models is imperative to ensure evaluation reliability, which makes conventional multi-objective optimization procedures prohibitively expensive. The employment of fast surrogates (or metamodels) can alleviate these difficulties, yet, construction of metamodels faces considerable challenges by itself, mostly related to the curse of dimensionality. This work proposes a novel surrogate-assisted approach to multi-objective optimization, where the data-driven model is only rendered in a small region spanned by the selected principal components of the extreme Pareto-optimal design set obtained using local search routines. The region is limited in terms of parameter ranges but also dimensionality, yet contains the majority of Pareto front, therefore surrogate construction therein does not incur considerable costs. The typical cost of identifying the Pareto set is just a few hundred of full-wave analyses of the antenna under design. Our technique is validated using two antenna examples (a planar Yagi and an ultra-wideband monopole antenna) and favorably compared to state-of-the-art surrogate-assisted multi-objective optimization methods.

INDEX TERMS Antenna design, multi-objective optimization, surrogate modeling, domain confinement, principal components, dimensionality reduction.

I. INTRODUCTION

Design of modern antenna structures faces several serious challenges. These arise from the necessity of satisfying stringent requirements pertinent to electrical and field characteristics (e.g., broadband operation [1], pattern stability [2], circular polarization [3]), implementation of various functionalities (e.g., multi-band operation [4], band notches [5], pattern diversity [6]), demands pertinent to emerging application areas (5G [7], internet of things [8]), but also small physical size [9], [10], critical for wearable [11] or implantable devices [12]. A fulfilment of such demands leads to the development of topologically complex antenna structures described by a large number of geometry parameters [13]–[15]. Their design, in particular, parameter tuning, is hindered by the necessity of handling several objectives

The associate editor coordinating the review of this manuscript and approving it for publication was Frederico Guimarães.

and constraints over highly-dimensional parameter spaces. For reliability reasons, antenna evaluation needs to be carried out through full-wave electromagnetic (EM) analysis, which creates an even more serious bottleneck. Furthermore, the design objectives are often conflicting so that it is not possible to improve all of them simultaneously, and compromise (trade-off) solutions have to be sought. Design of compact antennas provides a representative example. Reduction of the radiator size leads to a variety of issues, in particular, difficulties in ensuring sufficient matching (especially for broadband antennas) as well as degradation of other characteristics including gain, efficiency, and pattern stability [16], [17]. Depending on the designer's priorities, antenna performance with respect to some of these figures may be compromised in exchange for the improvement of others.

Needless to say, traditional simulation-based design methods, largely relying on supervised parameter sweeping, are unable to handle multiple goals and constraints. This can only be realized through rigorous numerical optimization [18]. However, most of widely used algorithms, including conventional methods (e.g., gradient-based [19] or pattern search [20]) or computational-intelligence-based techniques (e.g., evolutionary algorithms [21], particle swarm optimizers [22], or differential evolution [23]) are single-objective routines that can only process scalar cost functions. Controlling several objectives requires either aggregation (e.g., by means of a weighted sum method [24]), or turning most of the objectives (typically, all but one) into constraints and assigning appropriate acceptance levels. Regardless of the approach, single-objective optimization yields a design that corresponds to the designer's priorities concerning the considered goals.

Obtaining more comprehensive information about available design trade-offs requires genuine multi-objective optimization (MO), the outcome of which is typically a Pareto set pertinent to the design task at hand [25]. Although single-objective routines may be used to yield the Pareto set, e.g., through multiple minimization of an aggregated cost function with varying weighting factors [24], the most popular techniques these days are multi-objective versions of population-based metaheuristics [26]–[29]. Their advantage is a capability of producing the entire Pareto set within a single algorithm run. In antenna design, the algorithms belonging to this group are most often utilized for antenna array synthesis to adjust the array element spacing and determine the excitation tapers. The optimization is normally executed at the level of analytical array factor models. The numerous examples include artificial bee colony algorithm [30], grasshopper optimizer [31], ant lion algorithm, cat swarm optimizer, and whale optimizer [32], dragonfly algorithm [33], invasive weed algorithm [34] and particle swarm optimization [35]. The application of the latter for design optimization of antenna structure simulated in time-domain can also be found in [36], yet, the antenna structure was a simple one, and comprised a limited number of predefined segments. Comprehensive reviews and juxtaposition of the aforementioned algorithms can be found in [37]–[42].

A disadvantage of population-based methods is high computational cost, which often turns prohibitive when full-wave EM analysis needs to be employed to evaluate antenna characteristics. Therefore, number of practical applications of metaheuristics for solving directly EM-based optimization tasks is scarce and the reported overall optimization costs are high: from few hours [43] to several hundred hours [44].

Among available means of alleviating the aforementioned difficulties, in particular, making EM-based multi-objective optimization practical in computational terms, utilization of surrogate modeling techniques seems to be the most promising [45]. In particular, surrogate methods are used in conjunction with methaheuristic methods for design of antennas and microwave devices [46]–[50]. Applicability of surrogates very much depends on the particular problem. As long as the parameter space dimensionality is low and the system responses are not highly nonlinear, it might be possible to construct a global metamodel as an overall replacement of EM simulations [51]–[53]. As a matter of fact, it should be observed that in the aforementioned works [46]–[50], only low-dimensional problems were considered, with the structures under design described by few parameters (from two to six). Unfortunately, design of modern antennas often requires handling at least medium number of parameters (>10), where rendering reliable surrogate within the entire space is not possible. A viable alternative is an appropriate confinement of the search space along with the employment of variable-fidelity EM simulations [54], [55]. The keystone here is an identification of the region encapsulating the Pareto front and a construction of the replacement model therein. This approach demonstrably yields significant computational benefits [55] despite the fact that the space reduction techniques usually provide only a rough approximation of the Pareto front.

Constructing the surrogate model only in the region containing the Pareto front allows for a partial alleviation of the dimensionality problem and for improving the computational efficiency of the multi-objective optimization process. In [25], the encapsulation of the Pareto front has been achieved based on the extreme Pareto-optimal designs produced through single-objective optimization runs (one objective at the time), which gives an idea about the span of the front. More involved methods such as constrained modeling techniques (e.g., [56]) allow for more precise front allocation, and further computational advantages. This paper proposes a novel framework for multi-objective design optimization of antenna structures that capitalizes on performance-driven surrogate modeling concept [57], as well as explicit reduction of the parameter space dimensionality based on the principal component analysis (PCA) [58] of the extreme Pareto-optimal designs. The main purpose and the scope of the work is to yield further advantages over the methods involving the surrogates set up in constrained domain, specifically [25] and [56]. Here, the surrogate is constructed in the region containing the Pareto set and permits low-cost

identification of the best trade-off designs, further refined using local routines (also surrogate-assisted). Excellent accuracy of the replacement model obtained using small training data sets ensures efficiency without involving variable-fidelity EM simulations. Our methodology is demonstrated using a planar quasi-Yagi antenna designed for best matching and maximum gain, as well as an ultra-wideband monopole designed for best matching, minimum in-band gain variability, and minimum footprint area. The Pareto sets are rendered at the cost of a few hundred of EM analyses of the respective antenna structures. The computational savings compared to the benchmark surrogate-assisted technique exceeds 80 percent. The originality and major novel contributions of this work include: (i) development of computationally-efficient procedure for multi-objective antenna optimization, (ii) incorporation of the performance-driven modeling concept and PCA-based dimensionality reduction mechanisms into surrogate-assisted multi-objective design framework that allows for initial approximation of the Pareto set (this includes introduction of a rigorous formalism), as well as (iii) demonstration of the efficacy of the resulting MO procedure when handling real-world antenna design tasks as well as its superiority over state-of-the-art surrogate-assisted procedures.

II. SURROGATE-ASSISTED MULTI-OBJECTIVE ANTENNA OPTIMIZATION WITH DIMENSIONALITY REDUCTION

This section formulates the proposed multi-objective optimization (MO) methodology. First, some background material is discussed, in particular, a generic procedure for surrogate-assisted MO (Section II.*A*), followed by the concept of parameter space confinement (Section II.*B*). Section II.*C* presents a construction of surrogate model constrained to a reduced-dimensionality domain, defined using the principal components of the extreme Pareto-optimal design set. The overall operation of the proposed MO procedure is explained in Section II.*D* and illustrated using a flow diagram.

A. SURROGATE-BASED MULTI-OBJECTIVE DESIGN: GENERIC PROCEDURE

Let us denote the design goals as F_k, $k = 1, \ldots, N_{obj}$, with N_{obj} being the overall number of the objectives. In this work, the purpose of multi-objective optimization (MO) is understood as an identification of a globally non-dominated set of solutions (a so-called Pareto set) [59]. A formal definition of a dominance relation can be found in [25] but loosely speaking, a non-dominated design (also referred to as a Pareto optimal point) has the following property: within the considered parameter space there is no other design that would be simultaneously better with respect to all objectives. Hence, all elements of the Pareto set are equally good in the MO sense and represent the best possible trade-offs with respect to the objective vector $[F_1 F_2 \ldots F_{Nobj}]^T$.

The output of the computational model of the antenna will be denoted as $\boldsymbol{R}(\boldsymbol{x})$, where $\boldsymbol{x}$ represents adjustable parameters (most often, selected antenna dimensions). In most practical cases, full-wave EM analysis is employed for antenna evaluation, therefore, conducting MO directly at the level of $\boldsymbol{R}$ entails significant computational expenses. This is especially when MO is realized using population-based metaheuristic algorithms. Perhaps the most promising approach to mitigating this issue is surrogate-assisted approach [45], [51]–[53] (see also Section I), where the computational burden is shifted towards a faster representation of the antenna at hand, the surrogate model $\boldsymbol{R}_s$. Typically, it is a data-driven model, for example kriging [60], Gaussian process regression (GPR) [61], or neural network [45]. Because the evaluation cost of the surrogate is negligible as compared to EM analysis, $\boldsymbol{R}_s$ can be optimized directly using, for example, multi-objective evolutionary algorithms [62] or MO version of any of popular metaheuristics. At this point, it should be mentioned that several surrogate-based techniques that do not rely on population-based methods to yield a Pareto set have been recently developed (e.g., [63], [64]).

Additional reduction of the computational cost can be obtained by using variable-fidelity EM simulations. One of possible realizations is to construct the surrogate at the level of coarse-discretization EM model [54], [55]. This renders considerable savings (acquisition of the training data is the single most expensive component of the optimization procedure) but requires an additional refinement step in order to account for the misalignment between the low- and high-fidelity models. The refinement process can be conducted by means of output space mapping (OSM) [65]. More specifically, the high-fidelity designs are found as

$$\boldsymbol{x}_f^{(k)} = \arg \min_{\substack{\boldsymbol{x},\ F_2(\boldsymbol{x}) \le F_2(\boldsymbol{x}_s^{(k)}) \\ \vdots \\ F_{N_{obj}}(\boldsymbol{x}) \le F_{N_{obj}}(\boldsymbol{x}_s^{(k)})}} F_1\left(\boldsymbol{R}_s(\boldsymbol{x}) + [\boldsymbol{R}(\boldsymbol{x}_s^{(k)}) - \boldsymbol{R}_s(\boldsymbol{x}_s^{(k)})]\right) \tag{1}$$

In (1), $\boldsymbol{x}_f^{(k)}$ and $\boldsymbol{x}_s^{(k)}$ denote the high- and low-fidelity Pareto optimal designs, $k = 1, \ldots, N_{obj}$, respectively, and $\boldsymbol{R}(\boldsymbol{x}_s^{(k)}) - \boldsymbol{R}_s(\boldsymbol{x}_s^{(k)})$ represents the OSM term. The process is executed for low-fidelity Pareto-optimal designs $\boldsymbol{x}_s^{(k)}$ selected from the initial Pareto set generated using $\boldsymbol{R}_s$. In (1), the OSM term $\boldsymbol{R}(\boldsymbol{x}_s^{(k)}) - \boldsymbol{R}_s(\boldsymbol{x}_s^{(k)})$ ensures zero-order consistency [66] between the surrogate $\boldsymbol{R}_s$ and the high-fidelity model at $\boldsymbol{x}_s^{(k)}$. An alternative way of realizing the refinement process has been proposed in [67] using co-kriging, where the high-fidelity data sparsely sampled along the Pareto front is directly incorporated into the surrogate model. It should also be emphasized that—due to limited accuracy of the surrogate model—the refinement procedure may be required even if single-fidelity simulations are used in the MO process.

B. INITIAL PARAMETER SPACE CONFINEMENT

Except some simple cases (e.g., antenna described by a few parameters within narrow ranges thereof), a construction of surrogate model in the entire parameter space is most often

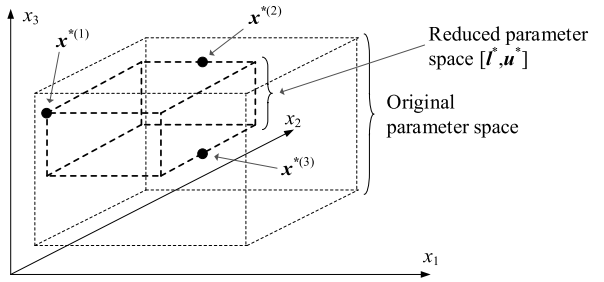

FIGURE 1. Parameter space reduction using single-objective optima $x^{*(k)}$ (cf. (2)).

hindered by the curse of dimensionality. At the same time, it is not necessary as the Pareto-optimal designs normally occupy a small portion of the space. A reasonable way of reducing parameter ranges is to consider the extreme Pareto-optimal points, corresponding to single-objective optima

$$\boldsymbol{x}^{*(k)} = \arg\min_{\boldsymbol{x}} F_k\left(\boldsymbol{R}(\boldsymbol{x})\right) \tag{2}$$

In (2), $\boldsymbol{x}^{*(k)}$ refers to the extreme design, i.e., design optimized with the use of single-objective optimization algorithm in the reduced parameter space, defined as an interval $[\boldsymbol{l}^*, \boldsymbol{u}^*]$ that normally contains the majority of the Pareto front. The narrowed lower $\boldsymbol{l}^*$ and upper $\boldsymbol{u}^*$ bands are defined as: $\boldsymbol{l}^* = \min\{\boldsymbol{x}^{*(1)},\ldots, \boldsymbol{x}^{*(Nobj)}\}$ and $\boldsymbol{u}^* = \max\{\boldsymbol{x}^{*(1)},\ldots, \boldsymbol{x}^{*(Nobj)}\}$, respectively [25] (see Fig. 1). Hence, it is sufficient to set up the surrogate model therein. More involved reduction techniques may provide even better confinement. An example is the parameter space reduction by means of nested kriging [68].

C. SURROGATE MODEL DOMAIN SETUP USING PRINCIPAL COMPONENTS

In this work, as a way of further improving computational efficiency of the MO process, the aim is to establish the domain of the surrogate model that provides more efficient parameter space confinement than the reduction technique described in Section II.*B*. The domain should contain a possibly large portion of the Pareto front and it should exhibit simple geometry so that identification of the Pareto set therein is straightforward.

The initial information about the Pareto front allocation is provided by the extreme designs $\boldsymbol{x}^{*(k)}$ of (2). Additional data, necessary to account for the front curvature, may be obtained by considering the designs

$$\boldsymbol{x}^{\boldsymbol{w}} = \arg\min_{\boldsymbol{x}} \sum_{k=1}^{N_{obj}} w_k F_k\left(\boldsymbol{R}(\boldsymbol{x})\right) \tag{3}$$

where $\boldsymbol{x}^{\boldsymbol{w}}$ denotes the supplemental design obtained for the weight vector $\boldsymbol{W} = [w_1 \ldots w_{Nobj}]^T$, with $w_k, k = 1, \ldots, N_{obj}$, being the weighting factors forming the convex combination of the objectives, i.e.,

$$0 \le w_k \le 1 \quad \text{and} \quad \sum\nolimits_{k=1}^{N_{obj}} w_k = 1 \tag{4}$$

Clearly, the extreme designs $\boldsymbol{x}^{*(k)}$ are solutions of (3) for $\boldsymbol{W} = [0 \ldots 1 \ldots 0]^T$ with 1 on the kth position. The design obtained for $\boldsymbol{W} = [1/N_{obj}\ 1/N_{obj} \ldots 1/N_{obj}]^{\mathrm{T}}$ corresponds to (more or less) the front center. Let us denote as $\{\boldsymbol{x}^{\boldsymbol{w}k}\}$, $k = 1, \ldots, p$, the set of all designs generated for the purpose of surrogate model establishment.

The model domain is defined using spectral analysis of the set $\{\boldsymbol{x}^{\boldsymbol{w}k}\}$ according to the description below. Let also denote as $\boldsymbol{x}_m = p^{-1}\sum_{k=1,\ldots,p}\boldsymbol{x}^{\boldsymbol{w}k}$ the center of gravity of $\{\boldsymbol{x}^{\boldsymbol{w}k}\}$. Let also C refer to the covariance matrix of the set

$$\boldsymbol{C} = \frac{1}{p-1}\sum_{k=1}^{p}(\boldsymbol{x}^{\boldsymbol{w}_k} - \boldsymbol{x}_m)(\boldsymbol{x}^{\boldsymbol{w}_k} - \boldsymbol{x}_m)^T \tag{5}$$

Let us also introduce as $\boldsymbol{v}_k$ the eigenvectors of the set $\{\boldsymbol{x}^{\boldsymbol{w}k}\}$ and as λ_k their counterpart eigenvalues. The pairs $\{\boldsymbol{v}_k, \lambda_k\}$, $k = 1, \ldots, p-1$, comprise the eigenvectors (i.e., the principal components) of $\{\boldsymbol{x}^{\boldsymbol{w}k}\}$ and their corresponding eigenvalues. The latter are the variances of $\{\boldsymbol{x}^{\boldsymbol{w}k}\}$ in the eigenspace. The eigenvalues are assumed to be ordered, i.e., $\lambda_1 \ge \lambda_2 \ge \ldots \ge \lambda_{p-1} \ge 0$. The matrix $\boldsymbol{V}_K = [\boldsymbol{v}_1 \ldots \boldsymbol{v}_K]$ consists of the first K eigenvectors as columns, K being the selected number of the principal directions.

The information carried by the matrix $\boldsymbol{V}_K$ will be used to define the surrogate model domain X_S. In particular, the domain is to be spanned with the use of the most dominant principal components, the number of which can be determined through the analysis of the eigenvalues. Typically, the eigenvalues are quickly decreasing so that it is sufficient to use $K = 3$ or 4 without missing any important information about the antenna at hand. The details will be provided in Section III when discussing specific application examples.

The process of defining the model domain involves expansion of the vectors $\boldsymbol{x}^{\boldsymbol{w}k}$ with respect to the principal components

$$\bar{\boldsymbol{x}}^{\boldsymbol{w}_k} = \boldsymbol{x}_m + \sum\nolimits_{j=1}^{p} b_{kj}\boldsymbol{v}_j \tag{6}$$

where the bar indicates that the left-hand-side of (6) is the part of $\boldsymbol{x}^{\boldsymbol{w}k}$ that is contained in the affine space spanned by $\boldsymbol{x}_m$ and $\boldsymbol{V}$. The coefficients b_{kj} are calculated as $b_{kj} = \boldsymbol{v}_j[\boldsymbol{v}_j^T(\boldsymbol{x}^{\boldsymbol{w}k} - \boldsymbol{x}_m)]$. The following notation is used

$$b_{j.\max} = \max\{k : b_{kj}\}, \quad b_{j.\min} = \min\{k : b_{kj}\} \tag{7}$$

$$b_{j.0} = \frac{b_{j.\min} + b_{j.\max}}{2}, \quad j = 1, \ldots, p \tag{8}$$

$$\boldsymbol{b}_0 = \left[b_{1.0}\ \ldots\ b_{p.0}\right]^T \tag{9}$$

and

$$\boldsymbol{\lambda}_{\boldsymbol{b}} = \left[\lambda_{b1}\ \ldots\ \lambda_{bp}\right]^T \tag{10}$$

In (9), $\boldsymbol{b}_0$ is the coefficient matrix whose entries are given by (8). Whereas the entries of the matrix $\lambda_{\boldsymbol{b}}$ are defined as $\lambda_{bj} = (b_{j.\max} - b_{j.\min})/2$ (cf. (7)). The domain X_S of the surrogate model is determined w.r.t. the center point

$$\boldsymbol{x}_c = \boldsymbol{x}_m + \boldsymbol{V}\boldsymbol{b}_0 \tag{11}$$

Using the above, one can define

$$X_k = \left\{ \begin{array}{c} \boldsymbol{x} = \boldsymbol{x}_c + \sum_{j=1}^{K} (2\lambda_j - 1)\lambda_{b_j} \boldsymbol{a}_j \\ 0 \le \lambda_j \le 1, \quad j = 1, \ldots, K \end{array} \right\} \tag{12}$$

It should be noted that X_K, i.e., the constrained domain of the dimensionality K, contains the entire set $\{\boldsymbol{x}^{wk}\}$ (in the directions $\boldsymbol{v}_1$ through $\boldsymbol{v}_k$). The surrogate model domain is defined as $X_S = X_K$ for a specific value of K selected by the user. As mentioned before, due to high correlation between optimum sets of antenna geometry parameters across the objective space, K equal to 3 or 4 is usually sufficient. Increasing this number does not bring much of useful information while being detrimental to the computational benefits achieved by dimensionality reduction. A graphical illustration of the concepts discussed in this section can be found in Fig. 2.

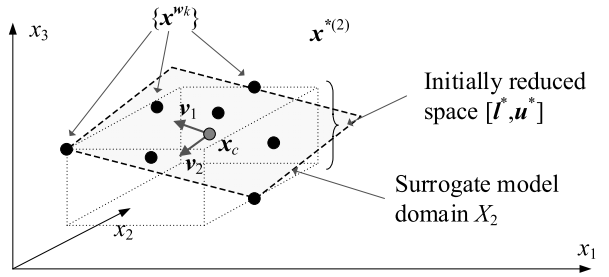

FIGURE 2. Graphical illustration of the surrogate model definition (here, two-dimensional X_2) for the purpose of constructing the surrogate model with the MO framework. The domain is spanned by the two most dominant principal components of the set $\{x^{wk}\}$.

Having the domain X_S, the surrogate model is obtained using kriging interpolation [69]. Design of experiments is arranged as follows. In order to achieve uniform allocation of the training data, an improved Latin Hypercube Sampling (LHS) procedure is used [70], with the samples $\boldsymbol{z} = [z_1 \ldots z_K]^T$ initially distributed in a normalized interval $[0\ 1] \times \ldots \times [0\ 1]$, i.e., $0 \le z_j \le 1$, $j = 1, \ldots, K$. Subsequently, the samples are mapped into X_S using the transformation

$$\boldsymbol{y} = h(\boldsymbol{z}) = \boldsymbol{x}_c + \sum_{j=1}^{K} (2z_j - 1)\lambda_{b_j} \boldsymbol{v}_j \tag{13}$$

where λ_{bj} are the coefficients defined in (10), and $\boldsymbol{v}_j$ are the eigenvectors of the set $\{\boldsymbol{x}^{wk}\}$. Whereas h refers to the surjective transformation from the unity hypercube into the constrained domain X_S.

D. PROPOSED MULTI-OBJECTIVE DESIGN FRAMEWORK

The operation of the proposed MO framework can be summarized as follows. The first stage of the optimization process is identification of the extreme Pareto optimal designs using single-objective optimization runs as described in Section II.*C* (equations (3) and (4)). Using the spectral analysis of this data, the domain of the surrogate model is established (cf. (12)), and the model is constructed upon acquiring the training data $\{\boldsymbol{x}_B^{(j)}, \boldsymbol{R}(\boldsymbol{x}_B^{(j)})\}, j = 1, \ldots, N_B$.

Subsequently, the initial approximation of the Pareto set is found using multi-objective evolutionary algorithm (MOEA) [62] operating directly on the surrogate model. Finally, selected Pareto-optimal designs are refined as described in Section II.*A* (eq. (1)). The flow diagram of the procedure has been shown in Fig. 3.

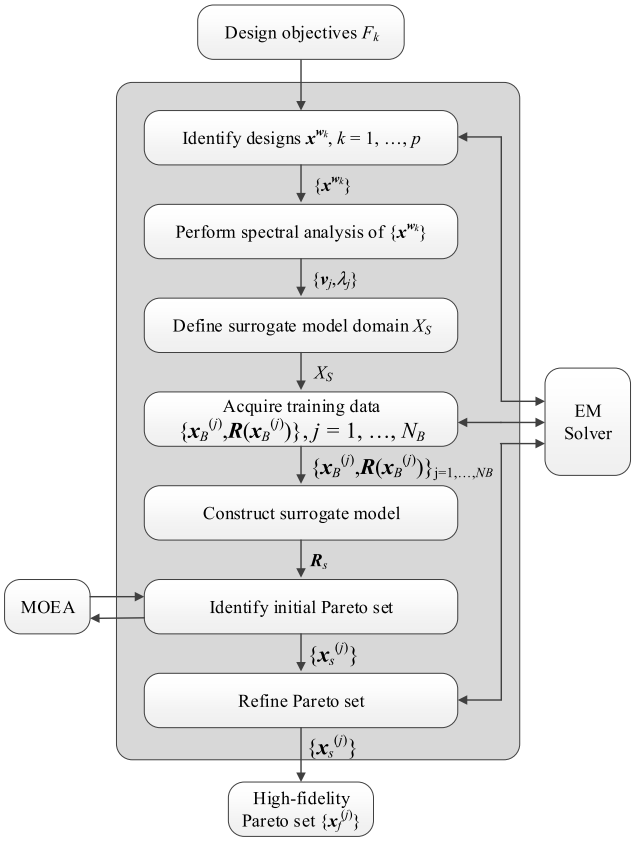

FIGURE 3. Flow diagram of the proposed multi-objective optimization procedure.

A few comments should be made concerning optimization of the surrogate model. The surrogate is defined over the domain X_S and all operations (including identification of the initial Pareto set using MOEA) should be carried out within X_S. For the sake of convenience, the optimization is formally conducted in the unity interval $[0,1] \times \ldots \times [0,1]$, whereas evaluation of the model is carried out using the auxiliary mapping $h : [0,1]^K \rightarrow X_S$ (cf. (13)).

It should be mentioned that the overall multi-objective optimization framework proposed in this work does not really have any control parameters that would have to be tuned by the user. The particular stages of the optimization process (acquisition of the reference points, surrogate model domain definition, surrogate model construction, rendering initial Pareto set, design refinement) are uniquely determined. For example, the reference points are obtained through single-objective optimization runs and there is nothing here that

the user might want to interfere with. The surrogate model is constructed to ensure good predictive power; say, around 5-percent of relative root mean square (RMS) error, and the number of training data samples is adjusted accordingly. The MOEA setup is made redundant to ensure that the variance of approximating the initial Pareto set is low (see the comments in the second paragraph of Section III). Thus, assuming that all algorithmic building blocks of the overall procedure are set up in a reasonable manner, there is nothing for the user to set up about the entire procedure, other than the number of Pareto-optimal points he/she might want to produce as the final outcome of the algorithm.

III. VERIFICATION STUDIES AND BENCHMARKING

For demonstration purposes, the proposed multi-objective optimization procedure has been validated using two antenna examples, a planar Yagi and an ultra-wideband (UWB) monopole. The structures were optimized for two and three objectives, respectively. In the case of Yagi antenna, the objectives are improvement of the in-band matching and maximization of the average end-fire gain. Whereas for the monopole, the goals are matching improvement, reduction of the in-band gain variability, and reduction of the antenna footprint. The benchmark algorithm was a generic surrogate-assisted framework described in Section II.*A* with the initial parameter space reduction of Section II.*B*. Here, all algorithms were exclusively using high-fidelity EM simulations (no variable-fidelity models involved). It should be emphasized that the very setup of all considered methods (the proposed one and the benchmark) ensures that that comparison is fair: all technique share the same reference designs, MOEA algorithm setup, as well as the refinement scheme. The only, yet fundamental, difference is the way of constraining and defining the surrogate model domain.

The results presented below were obtained based on single runs of the optimization algorithm. This is because most of the stages of the algorithm are deterministic, including identification of the reference designs for surrogate model domain definition, the domain definition itself, as well as the design refinement procedure (1). The only optimization stage that has a stochastic nature is multi-objective evolutionary algorithm (MOEA) used to generate the initial approximation of the Pareto set. However, MOEA operates on the fast surrogate and it is set up to use a large population (here, 1,000 individuals) and run for a few hundred iterations, both to minimize possible front deviations due to stochastic component of the search process. As indicated in [25] (Chapter 10.2), this setup allows for obtaining very small deviations of the Pareto front between algorithm runs (at the level of a small fraction of dB for the reflection or gain characteristics), which virtually eliminates the need for repeating the runs in practical application of the method.

A. EXAMPLE 1: PLANAR YAGI ANTENNA

Our first test case is a planar Yagi antenna [71]. The geometry of the structure has been shown in Fig. 4 and contains a driven

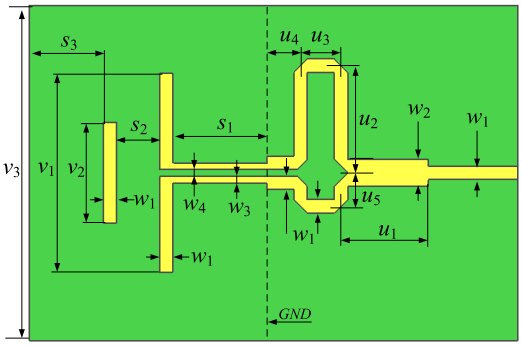

FIGURE 4. Geometry of the planar Yagi antenna. The ground plane extends until the dashed vertical line marked *GND*. Metallization marked using the yellow color.

element and a microstrip balun. The antenna is implemented on RT6010 substrate ($\varepsilon_r = 10.2$, $h = 0.635$ mm). There are eight designable parameters: $\boldsymbol{x} = [s_1\ s_2\ v_1\ v_2\ u_1\ u_2 u_3\ u_4]^T$. Other parameter are fixed: $w_1 = w_3 = w_4 = 0.6$, $w_2 = 1.2$, $u_5 = 1.5$, $s_3 = 3.0$ and $v_3 = 17.5$. All dimensions are in millimeters. The EM simulation model $\boldsymbol{R}$ is implemented in CST Microwave Studio (~600,000 mesh cells, simulation time 4 minutes) and evaluated using its time domain solver.

The operating frequency range of the antenna is 10 GHz to 11 GHz. The design objectives are minimization of in-band reflection (F_1) and maximization of the average end-fire gain (F_2), both within the operating bandwidth.

There are two extreme Pareto-optimal designs obtained to set up the surrogate model domain, $\boldsymbol{x}^{w1} = \boldsymbol{x}^{*(1)} = [4.43\ 3.85\ 8.77\ 4.28\ 4.09\ 4.76\ 2.08\ 1.63]^T$, $\boldsymbol{x}^{w2} = \boldsymbol{x}^{*(2)} = [5.19\ 6.90\ 7.10\ 5.08\ 3.54\ 4.78\ 2.23\ 0.93]^T$, and two additional points: $\boldsymbol{x}^{w3} = [4.56\ 4.38\ 8.56\ 4.50\ 3.89\ 4.93\ 2.01\ 1.57]^T$, $\boldsymbol{x}^{w4} = [4.84\ 5.00\ 8.09\ 4.64\ 3.98\ 4.89\ 2.00\ 1.50]^T$. These designs correspond to following weighting factors $[w_1 w_2]$ of (3), (4): [1 0], [0 1], [2/3 1/3], and [1/3 2/3].

The surrogate model was constructed using only 60 training samples and its relative RMS error is 1.5% and 0.8% for the reflection and gain characteristics, respectively. The model domain dimensionality is $K = 3$, which is the maximum number given four designs $\boldsymbol{x}^{wk}$. For comparison, the surrogate was also constructed in the initially reduced domain (cf. Section II. *A*), i.e., the interval $[\boldsymbol{l}^*\ \boldsymbol{u}^*]$ with $\boldsymbol{l}^* = \min\{\boldsymbol{x}^{*(1)}, \boldsymbol{x}^{*(2)}\}$ and $\boldsymbol{u}^* = \max\{\boldsymbol{x}^{*(1)}, \boldsymbol{x}^{*(2)}\}$. The error levels for this surrogate is much higher: 9% and 3% for reflection and gain, respectively, even though 1600 training samples were employed. For additional comparison, the surrogate was constructed using the nested kriging framework [56], one of the recent performance-driven modeling methods. Its domain was based on the same designs $\boldsymbol{x}^{*(k)}$, $k = 1, \ldots, 4$, and exhibits the error of 5% and 1% for the reflection and gain, respectively.

Figure 5 shows the initial Pareto set obtained by means of optimizing the surrogate model using multi-objective evolutionary algorithm [62]. The picture also shows ten designs

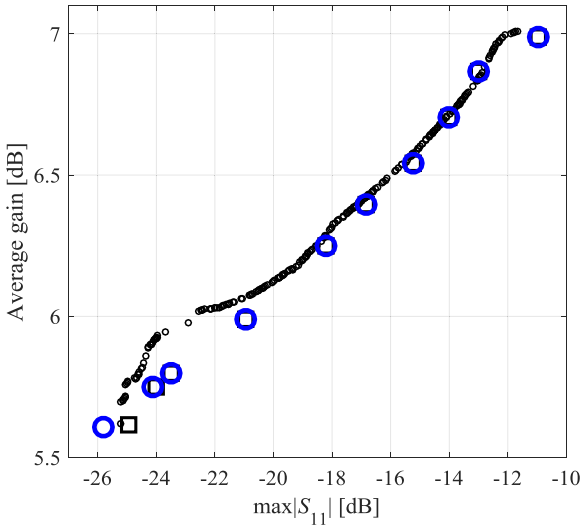

FIGURE 5. Planar Yagi antenna of Fig. 4: Pareto set identified using the proposed methodology: (o) initial set found by means of MOEA executed on the PCA-based surrogate, (□)designs selected from the initial Pareto set (EM simulation data), (O) refined Pareto-optimal designs (EM simulation data).

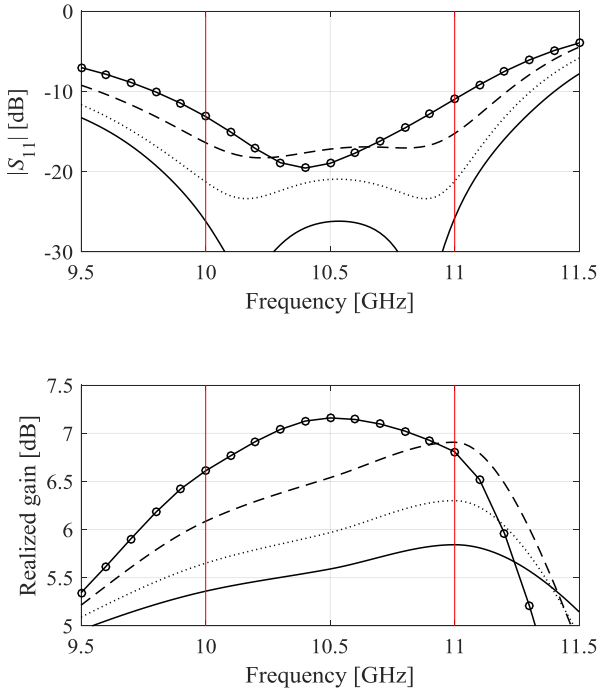

FIGURE 6. Planar Yagi antenna of Fig. 4: reflection (top) and end-fire gain (bottom) characteristics for the selected Pareto designs of Table 1: $\boldsymbol{x}^{(1)}$ (–),, $\boldsymbol{x}^{(4)}$ (· · ·), $\boldsymbol{x}^{(7)}$ (- - -), and $\boldsymbol{x}^{(10)}$ (-o-).

selected along the Pareto front before and after their refinement. Table 1 shows the antenna dimensions for the refined designs. The reflection and gain characteristics for a few designs have been illustrated in Fig. 6. Finally, Table 2 provides detailed information about the computational cost of the optimization process. Two benchmark methods are included in the table as well, both surrogate-assisted procedures: (i) the approach with surrogate model constructed in the initially reduced space, and (ii) the method involving the surrogate constructed with the nested kriging framework.

TABLE 1. Planar Yagi antenna: geometry parameter values for Pareto-optimal designs.

Design	Design Variables [mm]								max $\lvert S_{11}\rvert$ [dB]	Gain* [dB]
	s_1	s_2	v_1	v_2	u_1	u_2	u_3	u_4		
1	4.43	3.85	8.79	4.30	4.07	4.79	2.06	1.64	–25.8	5.6
2	4.45	3.91	8.79	4.35	4.01	4.88	2.01	1.66	–24.1	5.7
3	4.42	3.89	8.84	4.36	3.97	4.90	2.00	1.66	–23.5	5.8
4	4.56	4.40	8.56	4.50	3.88	4.92	2.02	1.56	–20.9	6.0
5	4.74	4.80	8.27	4.60	3.93	4.92	2.00	1.52	–18.2	6.2
6	4.82	5.05	8.09	4.65	3.93	4.88	2.03	1.46	–16.9	6.4
7	4.88	5.31	7.95	4.72	3.88	4.89	2.04	1.40	–15.2	6.5
8	4.97	5.64	7.76	4.80	3.83	4.88	2.06	1.32	–14.0	6.7
9	5.08	6.12	7.48	4.90	3.76	4.83	2.12	1.19	–13.0	6.9
10	5.17	6.68	7.26	5.09	3.54	4.92	2.12	1.05	–11.0	7.0

* End-fire gain averaged over the 10-to-11 GHz bandwidth.

TABLE 2. Yagi antenna: optimization cost and benchmarking.

Cost item	Surrogate model domain		
	X_S (this work)	X_S (nested kriging [56])	Hypercube $[\boldsymbol{l}^*,\boldsymbol{u}^*]$
Extreme points	$280 \times \boldsymbol{R}$	$280 \times \boldsymbol{R}$	$160 \times \boldsymbol{R}$
Data acquisition for kriging surrogate	$60 \times \boldsymbol{R}$	$100 \times \boldsymbol{R}$	$1600 \times \boldsymbol{R}$
MOEA optimization*	N/A	N/A	N/A
Refinement	$22 \times \boldsymbol{R}$	$30 \times \boldsymbol{R}$	$30 \times \boldsymbol{R}$
Total cost#	$362 \times \boldsymbol{R}$ (23 h)	$410 \times \boldsymbol{R}$ (27 h)	$1790 \times \boldsymbol{R}$ (118 h)

* The cost of MOEA optimization is negligible compared to other stages of the process.
# The total cost is expressed in terms of the equivalent number of EM simulations.

It can be observed that for the method operating within the initially reduced space, the major component of the overall cost is training data acquisition, which is greatly reduced for performance-driven modeling methods (from 1600 to 100 for the nested kriging and to only 60 samples for the proposed approach). Furthermore, due to very good accuracy of the surrogate model constructed as proposed in this work, the refinement process is considerably cheaper (for most designs it stops immediately as no improvement can be made). The overall cost is only 362 EM simulations.

It should be emphasized that the proposed approach allows for more accurate identification of the initial Pareto set, which is a result of a significantly smaller domain of the surrogate model. Figure 7 shows some comparative results. In particular, it can be observed that the Pareto front span obtained with the surrogate established in the initially reduced space is much smaller and the discrepancy between the initial and refined Pareto sets is significant. The latter is a result of limited accuracy of the surrogate model itself. The proposed approach renders the Pareto set of the same quality as that obtained using the nested kriging model, whereas the computational cost of the optimization process is smaller (362 versus 410 EM simulations, which give 12 percent speedup;

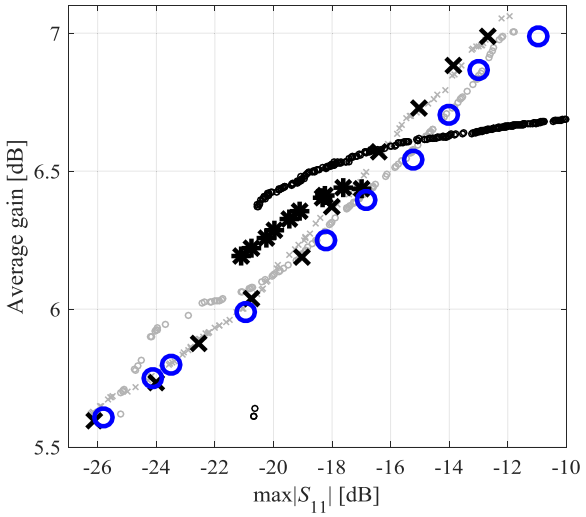

FIGURE 7. Planar Yagi antenna of Fig. 4. Initial Pareto sets obtained using: the surrogate-assisted procedure using initial design space reduction (surrogate constructed within the interval $[\boldsymbol{l}^*, \boldsymbol{u}^*]$) (black circles); the nested kriging surrogate (gray crosses); the proposed PCA-based surrogate (gray circles). EM-evaluated Pareto designs: refined points found in the interval $[\boldsymbol{l}^*, \boldsymbol{u}^*]$ (large stars ∗), refined Pareto designs found using the nested kriging (large black crosses ×), refined Pareto designs found using the proposed PCA-based surrogate (large blue circles). It should be noted that the span of the Pareto set obtained using performance-driven surrogates is considerable larger than for the surrogate constructed in the interval $[\boldsymbol{l}^*, \boldsymbol{u}^*]$ and the consistency between the initial and refined sets is improved (cf. Fig. 5). Also, the refined Pareto sets obtained using the nested kriging surrogate and the proposed surrogate are comparable, yet the proposed method offers reduced computational cost (cf. Table 2).

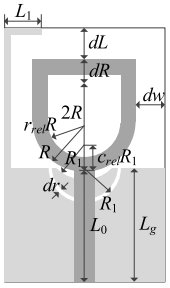

FIGURE 8. Ultrawideband monopole antenna [52]: structure geometry with the ground plane marked using the light gray shade.

however, if the cost of finding the extreme points is not included, the speedup becomes almost 40 percent).

B. EXAMPLE 2: ULTRA-WIDEBAND MONOPOLE ANTENNA

The second verification case study is the ultra-wideband monopole [72]. The antenna is implemented on RF-35 substrate ($\varepsilon_r = 3.5$, $h = 0.762$ mm). Its geometry, shown in Fig. 8, is described by eleven parameters $\boldsymbol{x} = [L_0\ dR\ Rr_{rel}\ dL\ dw\ L_g\ L_1R_1\ dr\ c_{rel}]^T$. The EM model is implemented in CST Microwave Studio and evaluated using its transient solver (∼840,000 mesh cells, simulation time 5 minutes). For reliability, the EM model incorporates the SMA connector.

The operating frequency range of the antenna is 3.1 GHz to 10.6 GHz. Three design objectives are considered: minimization of the in-band reflection (F_1), reduction of the realized gain variability within the operating frequency range (F_2), and reduction of the antenna footprint (F_3).

The domain of the surrogate model is established using seven designs. The first three are extreme Pareto-optimal designs corresponding to single-objective minima (best matching, minimum gain variation, and minimum size): $\boldsymbol{x}^{*(1)} = [10.64\ 0.0\ 6.00\ 0.10\ 1.46\ 6.20\ 10.46\ 4.26\ 2.00\ 0.73\ 0.49]^T$, $\boldsymbol{x}^{*(2)} = [8.74\ 1.55\ 5.81\ 0.51\ 0.016\ 5.65\ 8.95\ 5.47\ 2.60\ 0.99\ 0.84]^T$, $\boldsymbol{x}^{*(3)} = [9.51\ 0.19\ 4.46\ 0.27\ 4.33\ 1.17\ 10.05\ 6.00\ 2.94\ 0.99\ 0.90]^T$.

These points correspond to following weighting factors $[w_1\ w_2 w_3]$ of (3), (4): [1 0 0], [0 1 0], and [0 0 1]. There are four more points that correspond to $[w_1 w_2 w_3] = [0.5\ 0\ 0.5]$, [0.5 0.5 0], [0 0.5 0.5], and [1/3 1/3 1/3]: $\boldsymbol{x}^{*(4)} = [10.04\ 0.43\ 5.85\ 0.26\ 0.0\ 6.46\ 10.01\ 5.49\ 2.14\ 1.00\ 0.83]^T$, $\boldsymbol{x}^{*(5)} = [9.58\ 0.0\ 5.05\ 0.28\ 3.37\ 4.14\ 9.68\ 5.26\ 2.37\ 0.85\ 0.89]^T$, $\boldsymbol{x}^{*(6)} = [8.76\ 0.0\ 5.62\ 0.69\ 2.24\ 2.92\ 8.93\ 5.94\ 2.58\ 0.99\ 0.27]^T$, $\boldsymbol{x}^{*(7)} = [9.52\ 0.37\ 5.08\ 0.16\ 2.61\ 4.85\ 9.55\ 5.39\ 2.25\ 0.91\ 0.88]^T$.

The proposed surrogate has been set up using only 100 training samples. The domain dimension was set to $K = 4$ because of the eigenvalues of $\{\boldsymbol{x}^{wk}\}$, which are $\lambda_1 = 1.00$, $\lambda_2 = 0.22$, $\lambda_3 = 0.04$, $\lambda_4 = 0.03$, $\lambda_5 = 0.01$, and $\lambda_6 = 0.0007$ (normalized values). Thus, the last two principal directions are insignificant as compared to the dominant ones. The average RMS error of the surrogate is 5.2% and 4.5% for the reflection and gain characteristics, respectively. Similarly as for the previous example, the surrogate was also set up in the initially reduced space, i.e., the interval $\boldsymbol{l}^* = \min\{\boldsymbol{x}^{*(1)}, \boldsymbol{x}^{*(2)}, \boldsymbol{x}^{*(3)}\}$ and $\boldsymbol{u}^* = \max\{\boldsymbol{x}^{*(1)}, \boldsymbol{x}^{*(2)}, \boldsymbol{x}^{*(3)}\}$, using 1600 training samples. The error of this model is 15% (reflection) and 11% (gain). It should be emphasized that reliable modeling is hindered here by the parameter space dimensionality (eleven variables) but also relatively broad parameter ranges.

Additionally, the nested kriging model was set up using the designs $\{\boldsymbol{x}^{*(j)}\}_j = 1, \ldots, 7$, as the reference points [56]. Despite involving 200 data samples, the model error was 7.5% (reflection) and 5% (gain), which is not as good as for the proposed approach, mainly due to the dimensionality issues.

The initial Pareto set found by optimizing the proposed surrogate using multi-objective evolutionary algorithm, as well as the EM simulation data for the selected designs (before and after the refinement) has been illustrated in Fig. 9. The numerical data, including the geometry parameter values of the refined designs, has been gathered in Table 3. Figure 10 shows the reflection and realized gain characteristics for the selected designs from Table 3. Finally, the cost of the optimization process and its breakdown can be found in Table 4.

As it can be observed, acquisition of the training data is the largest contributor to the overall optimization cost for the benchmark method using the surrogate established in the initially reduced parameter space. The proposed approach reduces this part by the factor of sixteen, which leads to the overall speedup of almost 60 percent. This is achieved without compromising the quality of the Pareto front as shown in Fig. 11. The proposed approach also offers a certain cost

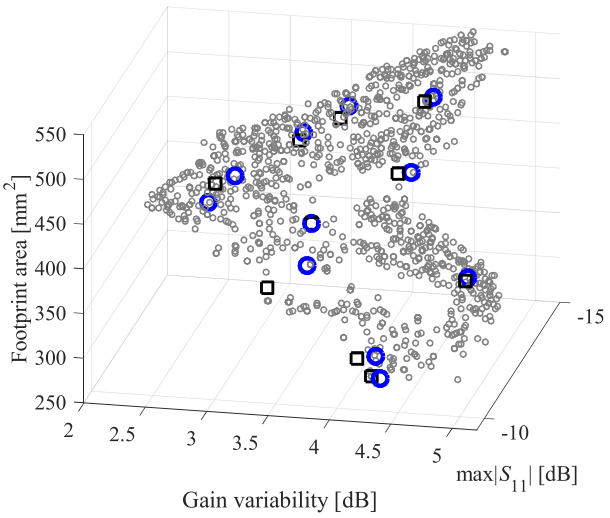

FIGURE 9. Ultrawideband monopole antenna of Fig. 8. Pareto-optimal solutions found using the proposed procedure: (o) initial Pareto set identified using multi-objective evolutionary algorithm executed on the proposed PCA-based surrogate, (□) EM-evaluated designs selected from the initial Pareto set, (O) EM-simulated refined Pareto designs.

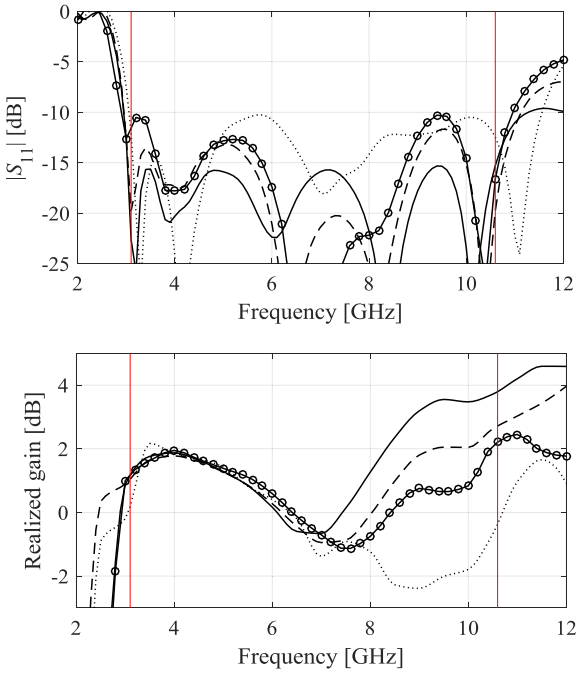

FIGURE 10. Ultrawideband monopole antenna of Fig. 8: reflection (top) and realized gain (bottom) responses for the selected Pareto-optimal designs of Table 3: $x^{(1)}$ (–), $x^{(3)}$ (· · ··), $x^{(5)}$ (- - -), and $x^{(10)}$ (-o-).

reduction as compared to the approach involving the nested kriging surrogate (about 10 percent), however, the reduction is over forty percent when the cost of finding the extreme Pareto optimal designs is excluded.

C. DISCUSSION

The numerical results obtained in Section III.*A* and III.*B* can be summarized as follows:

- The performance of the proposed MO procedure is consistent for both considered antenna structures different by the dimensionality of the parameter space and the number of objectives. In terms of variable and objective space complexity, these cases are representative for real-world situations and more complex than normally considered in the research papers on similar topics.
- The quality of the results is very similar for the proposed and the benchmark methods in terms of the Pareto set rendered during the optimization process. This allows for concluding that dimensionality reduction of the surrogate model domain does not have any detrimental effects on reliability.
- The methods selected as benchmark are state-of-the-art approaches for the class of algorithms considered within the scope of the paper (cf. Section I). The computational cost of the various stages of the MO process are therefore the same or comparable, except the surrogate modeling step, expediting of which was the very motivation for this work. Here, the proposed method offers a significant speedup of 40 and 50 percent with respect to nested kriging approach and well over 90 percent over the technique of [25]. This translates into significant acceleration of the entire procedure.

TABLE 3. Ultrawideband monopole antenna: geometry parameter values for Pareto-optimal designs.

Design		1	2	3	4	5	6	7	8	9	10	11	12
max $\|S_{11}\|$ [dB]		−15.3	−10.0	−10.3	−10.7	−11.7	−13.1	−11.1	−11.0	−13.7	−10.2	−10.9	−12.4
Gain variab. [dB]		4.5	3.0	4.6	3.3	3.7	3.9	5.5	4.4	4.4	3.3	4.2	4.4
Footprint [mm^2]		555	474	287	512	481	538	352	423	497	427	402	433
Design variables	L_0	10.0	9.25	8.93	9.21	9.74	9.40	9.03	9.26	9.74	8.72	8.89	9.37
	dR	0.49	0.20	0.12	0.49	0.55	0.88	0.12	0.00	0.29	0.68	0.36	0.20
	R	5.77	5.94	4.67	6.02	5.42	5.83	4.82	5.65	5.44	5.44	5.21	5.15
	r_{rel}	0.18	0.55	0.43	0.51	0.22	0.34	0.36	0.53	0.21	0.52	0.45	0.28
	dL	0.86	1.15	4.22	0.58	1.59	0.33	4.04	2.41	2.11	1.81	2.82	3.07
	Dw	6.50	4.75	1.77	5.61	5.31	6.42	2.99	3.67	5.50	4.37	3.84	4.42
	L_g	9.93	9.26	9.32	9.17	9.83	9.39	9.23	9.31	9.71	8.88	9.03	9.43
	L_1	4.91	5.44	5.98	5.35	5.27	5.23	5.56	5.48	5.01	5.69	5.57	5.22
	R_1	2.10	2.35	2.74	2.30	2.31	2.26	2.53	2.40	2.19	2.53	2.49	2.33
	dr	0.87	0.94	0.97	0.94	0.92	0.93	0.89	0.81	0.84	0.97	0.92	0.85
	c_{rel}	0.81	0.37	0.77	0.48	0.89	0.81	0.79	0.33	0.81	0.71	0.71	0.80

TABLE 4. Ultrawideband monopole antenna: optimization cost and benchmarking.

Cost item	Surrogate model domain		
	X_S (this work)	X_S (nested kriging [56])	Hypercube $[\boldsymbol{l}^*,\boldsymbol{u}^*]$
Extreme points	750 × $\boldsymbol{R}$	750 × $\boldsymbol{R}$	440 × $\boldsymbol{R}$
Data acquisition for kriging surrogate	100 × $\boldsymbol{R}$	200 × $\boldsymbol{R}$	1600 × $\boldsymbol{R}$
MOEA optimization*	N/A	N/A	N/A
Refinement	36 × $\boldsymbol{R}$	36 × $\boldsymbol{R}$	36 × $\boldsymbol{R}$
Total cost#	886 × $\boldsymbol{R}$ (73 h)	986 × $\boldsymbol{R}$ (82 h)	2076 × $\boldsymbol{R}$ (173 h)

* The cost of MOEA optimization is negligible compared to other stages of the process.
# The total cost is expressed in terms of the equivalent number of EM simulations.

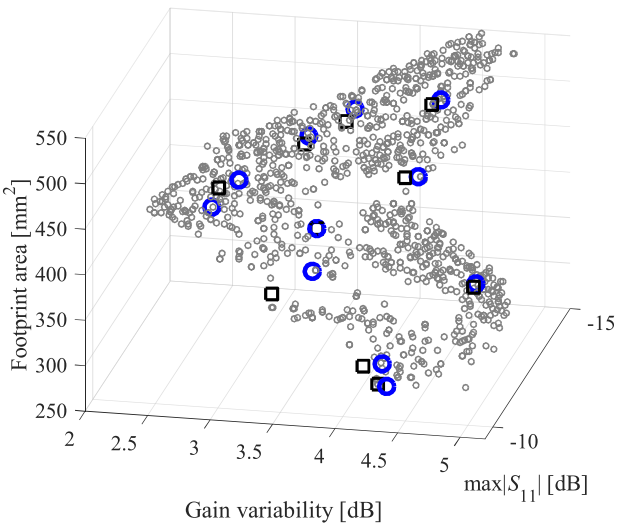

FIGURE 11. Ultrawideband monopole antenna of Fig. 8. Initial Pareto sets obtained using the approach proposed in this work (black circles) and with the surrogate model established in the initially reduced design space (the interval [$\boldsymbol{l}^*$, $\boldsymbol{u}^*$]) (gray circles). It should be noted that the Pareto front span is similar in both cases (slightly larger for the initially reduced space due to its considerably larger volume).

- The particular way of confining the surrogate model domain does not only result in reducing the number of training data samples required to construct reliable surrogate but also improves the model scalability, i.e., the relationship between the number of samples and the model predictive power. This allows for yielding the surrogates of excellent quality (a few percent of relative RMS error) using very small number of data samples. This can be viewed as an additional advantage of the approach.
- All considered methods (the proposed and the benchmark ones) employ the reference points in order to approximate the region of the parameter space containing the Pareto front. It requires certain initial investment in terms of the computational cost. It should be reiterated that this sort of investment is imperative for the test problem of this level of complexity, i.e., rendering the surrogates of any level of design utility without some sort of confinement (e.g., to the hypercube [$\boldsymbol{l}^*$, $\boldsymbol{u}^*$]) would not be possible.

The above comments allow us to draw the conclusion that the proposed approach fulfills the very purpose it was designed for, i.e., reduces the computational cost of one of the most expensive stages of the surrogate-assisted MO procedure of the class considered in this work, i.e., acquisition of the training data for surrogate model construction. The level of computational savings obtained by incorporating performance-driven modeling with dimensionality reduction is considerable and allows for accelerating the entire procedure without compromising the design quality.

The proposed multi-objective optimization framework is intended to be employed for real-world applications. Therefore, its implementation is made as simple as possible. This especially pertains to the fact that it does not require setting or adjusting any control parameters. The optimization process comprises the following deterministic stages: acquisition of the reference points (by means of single-objective optimization), defining the surrogate domain and constructing the model therein, rendering initial Pareto set and its refinement. In fact, the sole option that is left up to the user's discretion is the choice of the number of Pareto-optimal designs that are to be rendered as the final outcome of the algorithm.

IV. CONCLUSION

In the paper, a novel surrogate-based approach to multi-objective design optimization of antenna structures has been proposed. Our methodology involves a surrogate model constructed in a confined domain that is established using a set of Pareto-optimal designs obtained through single-objective optimization runs, and, more specifically, their principal components. This allows for identifying the parameter space region containing the Pareto front as well as reducing the domain dimensionality. The latter has a profound effect on the predictive power of the surrogate and a reduction of the computational cost of training data acquisition. The proposed approach has been comprehensively validated using two antenna examples, a planar Yagi antenna and a wideband monopole. In both cases, the 10- and 12-element Pareto sets have been rendered at the cost of a few hundred of EM simulations of the respective antenna structures, which yields a considerable savings as compared to the benchmark surrogate-assisted procedure (80 percent for the Yagi antenna and almost 60 percent for the monopole). At the same time, the presented approach has been demonstrated to produce the Pareto sets of the quality comparable to those obtained using the surrogate constructed within the recent nested kriging framework, which provides further cost reduction (up to twelve percent of the overall costs and forty percent of the surrogate modelling process). Our methodology can be considered a viable alternative for performing multi-objective design procedures in the cases where construction of conventional surrogates is hindered by the dimensionality and parameter range issues. Perhaps the most serious limitation of the approach is related to the dimensionality of the parameter space and the number of design objectives considered in the optimization process. Increasing either of them will have a detrimental effect on the quality of the surrogate model and will lead to the increase of the number of training data samples required to render reliable surrogate. This means, that for a sufficiently large number of parameters, the cost contribution of the training data acquisition will again become dominant (w.r.t. the overall cost). Also, the approach would may not work efficiently if the Pareto front is not connected, i.e., consists of several disjoint subsets. In such a case, the efficiency of the space reduction normally achieved using domain confinement will not be as advantageous as in the case of the (set-theory) connected Pareto front. Notwithstanding, the aforementioned issues are also pertinent to other surrogate-assisted approaches, and the proposed technique

allows for extending the range of application of surrogate-based optimization concept in terms of parameter space dimensionality as compared to conventional methods.

ACKNOWLEDGMENT

The authors would like to thank Dassault Systemes, France, for making CST Microwave Studio available.

REFERENCES

[1] T. Cheng, W. Jiang, S. Gong, and Y. Yu, "Broadband SIW cavity-backed modified dumbbell-shaped slot antenna," *IEEE Antennas Wireless Propag. Lett.*, vol. 18, no. 5, pp. 936–940, May 2019.

[2] Y. Wang and Z. Du, "Dual-polarized slot-coupled microstrip antenna array with stable active element pattern," *IEEE Trans. Antennas Propag.*, vol. 63, no. 9, pp. 4239–4244, Sep. 2015.

[3] U. Ullah and S. Koziel, "A broadband circularly polarized wide-slot antenna with a miniaturized footprint," *IEEE Antennas Wireless Propag. Lett.*, vol. 17, no. 12, pp. 2454–2458, Dec. 2018.

[4] J.-F. Qian, F.-C. Chen, K.-R. Xiang, and Q.-X. Chu, "Resonator-loaded multi-band microstrip slot antennas with bidirectional radiation patterns," *IEEE Trans. Antennas Propag.*, vol. 67, no. 10, pp. 6661–6666, Oct. 2019.

[5] Y. Xu, J. Wang, L. Ge, X. Wang, and W. Wu, "Design of a notched-band vivaldi antenna with high selectivity," *IEEE Antennas Wireless Propag. Lett.*, vol. 17, no. 1, pp. 62–65, Jan. 2018.

[6] Y. Dong, J. Choi, and T. Itoh, "Vivaldi antenna with pattern diversity for 0.7 to 2.7 GHz cellular band applications," *IEEE Antennas Wireless Propag. Lett.*, vol. 17, no. 2, pp. 247–250, Feb. 2018.

[7] Z. Nie, H. Zhai, L. Liu, J. Li, D. Hu, and J. Shi, "A dual-polarized frequency-reconfigurable low-profile antenna with harmonic suppression for 5G application," *IEEE Antennas Wireless Propag. Lett.*, vol. 18, no. 6, pp. 1228–1232, Jun. 2019.

[8] K. R. Jha, B. Bukhari, C. Singh, G. Mishra, and S. K. Sharma, "Compact planar multistandard MIMO antenna for IoT applications," *IEEE Trans. Antennas Propag.*, vol. 66, no. 7, pp. 3327–3336, Jul. 2018.

[9] X. Qin and Y. Li, "Compact dual-polarized cross-slot antenna with colocated feeding," *IEEE Trans. Antennas Propag.*, vol. 67, no. 11, pp. 7139–7143, Nov. 2019.

[10] A. A. Omar and Z. Shen, "A compact and wideband vertically polarized monopole antenna," *IEEE Trans. Antennas Propag.*, vol. 67, no. 1, pp. 626–631, Jan. 2019.

[11] S. Yan, P. J. Soh, and G. A. E. Vandenbosch, "Wearable dual-band magneto-electric dipole antenna for WBAN/WLAN applications," *IEEE Trans. Antennas Propag.*, vol. 63, no. 9, pp. 4165–4169, Sep. 2015.

[12] J. Wang, M. Leach, E. G. Lim, Z. Wang, R. Pei, and Y. Huang, "An implantable and conformal antenna for wireless capsule endoscopy," *IEEE Antennas Wireless Propag. Lett.*, vol. 17, no. 7, pp. 1153–1157, Jul. 2018.

[13] M. Borhani, P. Rezaei, and A. Valizade, "Design of a reconfigurable miniaturized microstrip antenna for switchable multiband systems," *IEEE Antennas Wireless Propag. Lett.*, vol. 15, pp. 822–825, 2016.

[14] J. L. Buckley, K. G. McCarthy, L. Loizou, B. O'Flynn, and C. O'Mathuna, "A dual-ISM-band antenna of small size using a spiral structure with parasitic element," *IEEE Antennas Wireless Propag. Lett.*, vol. 15, pp. 630–633, 2016.

[15] I. Szini, A. Tatomirescu, and G. F. Pedersen, "On small terminal MIMO antennas, harmonizing characteristic modes with ground plane geometry," *IEEE Trans. Antennas Propag.*, vol. 63, no. 4, pp. 1487–1497, Apr. 2015.

[16] J. Liu, K. P. Esselle, S. G. Hay, and S. Zhong, "Effects of printed UWB antenna miniaturization on pulse fidelity and pattern stability," *IEEE Trans. Antennas Propag.*, vol. 62, no. 8, pp. 3903–3910, Aug. 2014.

[17] S. Koziel, Q. S. Cheng, and S. Li, "Optimization-driven antenna design framework with multiple performance constraints," *Int. J. RF Microw. Comput.-Aided Eng.*, vol. 28, no. 4, May 2018, Art. no. e21208.

[18] E. Hassan, D. Noreland, R. Augustine, E. Wadbro, and M. Berggren, "Topology optimization of planar antennas for wideband near-field coupling," *IEEE Trans. Antennas Propag.*, vol. 63, no. 9, pp. 4208–4213, Sep. 2015.

[19] J. Wang, X.-S. Yang, and B.-Z. Wang, "Efficient gradient-based optimisation of pixel antenna with large-scale connections," *IET Microw., Antennas Propag.*, vol. 12, no. 3, pp. 385–389, Feb. 2018.

[20] T. G. Kolda, R. M. Lewis, and V. Torczon, "Optimization by direct search: New perspectives on some classical and modern methods," *SIAM Rev.*, vol. 45, no. 3, pp. 385–482, Jan. 2003.

[21] W.-J. Zhao, E.-X. Liu, B. Wang, S.-P. Gao, and C. E. Png, "Differential evolutionary optimization of an equivalent dipole model for electromagnetic emission analysis," *IEEE Trans. Electromagn. Compat.*, vol. 60, no. 6, pp. 1635–1639, Dec. 2018.

[22] A. Lalbakhsh, M. U. Afzal, and K. P. Esselle, "Multiobjective particle swarm optimization to design a time-delay equalizer metasurface for an electromagnetic band-gap resonator antenna," *IEEE Ant. Wireless Prop. Lett.*, vol. 16, pp. 912–915, 2017.

[23] S. K. Goudos and J. N. Sahalos, "Pareto optimal microwave filter design using multiobjective differential evolution," *IEEE Trans. Antennas Propag.*, vol. 58, no. 1, pp. 132–144, Jan. 2010.

[24] R. T. Marler and J. S. Arora, "The weighted sum method for multi-objective optimization: New insights," *Structural Multidisciplinary Optim.*, vol. 41, no. 6, pp. 853–862, Jun. 2010.

[25] S. Koziel and A. Bekasiewicz, *Multi-Objective Design of Antennas Using Surrogate Models*. Singapore: World Scientific, 2016.

[26] C. Zhang, X. Fu, X. Chen, S. Peng, and X. Min, "Synthesis of uniformly excited sparse rectangular planar array for sidelobe suppression using multi-objective optimisation algorithm," *J. Eng.*, vol. 2019, no. 19, pp. 6278–6281, Oct. 2019.

[27] P. Baumgartner, T. Bauernfeind, O. Biro, A. Hackl, C. Magele, W. Renhart, and R. Torchio, "Multi-objective optimization of Yagi–Uda antenna applying enhanced firefly algorithm with adaptive cost function," *IEEE Trans. Magn.*, vol. 54, no. 3, pp. 1–4, Mar. 2018.

[28] S.-H. Yang and J.-F. Kiang, "Optimization of sparse linear arrays using harmony search algorithms," *IEEE Trans. Antennas Propag.*, vol. 63, no. 11, pp. 4732–4738, Nov. 2015.

[29] S. K. Goudos, K. A. Gotsis, K. Siakavara, E. E. Vafiadis, and J. N. Sahalos, "A multi-objective approach to subarrayed linear antenna arrays design based on memetic differential evolution," *IEEE Trans. Antennas Propag.*, vol. 61, no. 6, pp. 3042–3052, Jun. 2013.

[30] C. Liu, F. Zheng, and C. Kai, "An improved multi-objective artificial bee colony algorithm for pattern synthesis of conformal arrays," in *Proc. 12th Int. Conf. Natural Comput., Fuzzy Syst. Knowl. Discovery (ICNC-FSKD)*, Changsha, China, Aug. 2016, pp. 265–270.

[31] H. Wang, C. Liu, H. Wu, B. Li, and X. Xie, "Optimal pattern synthesis of linear array and broadband design of whip antenna using grasshopper optimization algorithm," *Int. J. Antennas Propag.*, vol. 2020, Jan. 2020, Art. no. 5904018.

[32] H. Pradhan, B. B. Mangaraj, and S. Kumar Behera, "Antenna array optimization for smart antenna technology using whale optimization algorithm," in *Proc. IEEE Indian Conf. Antennas Propogation (InCAP)*, Ahmedabad, India, Dec. 2019, pp. 1–4.

[33] B. Babayigit, "Synthesis of concentric circular antenna arrays using dragonfly algorithm," *Int. J. Electron.*, vol. 105, no. 5, pp. 784–793, May 2018.

[34] Y. Liu, Y.-C. Jiao, Y.-M. Zhang, and Y.-Y. Tan, "Synthesis of phase-only reconfigurable linear arrays using multiobjective invasive weed optimization based on decomposition," *Int. J. Antennas Propag.*, vol. 2014, 2014, Art. no. 630529.

[35] S. K. Goudos, Z. D. Zaharis, D. G. Kampitaki, I. T. Rekanos, and C. S. Hilas, "Pareto optimal design of dual-band base station antenna arrays using multi-objective particle swarm optimization with fitness sharing," *IEEE Trans. Magn.*, vol. 45, no. 3, pp. 1522–1525, Mar. 2009.

[36] Z. Lukes and Z. Raida, "Multi-objective optimization of wire antennas: Genetic algorithms versus particle swarm optimization," *Radioengineering*, vol. 14, no. 4, pp. 91–97, 2005.

[37] P. Champasak, N. Panagant, N. Pholdee, S. Bureerat, and A. R. Yıldız, "Self-adaptive many-objective meta-heuristic based on decomposition for many-objective conceptual design of a fixed wing unmanned aerial vehicle," *Aerosp. Sci. Technol.*, vol. 100, May 2020, Art. no. 105783.

[38] H. Abderazek, A. R. Yıldız, and S. Mirjalili, "Comparison of recent optimization algorithms for design optimization of a cam-follower mechanism," *Knowl.-Based Syst.*, vol. 191, Mar. 2020, Art. no. 105237.

[39] A. R. Yıldız, H. Abderazek, and S. Mirjalili, "A comparative study of recent non-traditional methods for mechanical design optimization," *Arch. Comput. Methods Eng.*, vol. 27, no. 4, pp. 1031–1048, Sep. 2020, doi: 10.1007/s11831-019-09343-x.

[40] Z. Meng, G. Li, X. Wang, S. M. Sait, and A. R. Yıldız, "A comparative study of metaheuristic algorithms for reliability-based design optimization problems," *Arch. Comput. Methods Eng.*, pp. 1–17, 2020.

[41] S. Karagöz and A. R. Yıldız, "A comparison of recent metaheuristic algorithms for crashworthiness optimisation of vehicle thin-walled tubes considering sheet metal forming effects," *Int. J. Vehicle Des.*, vol. 73, nos. 1–3, pp. 179–188, 2017.

[42] B. S. Yıldız and A. R. Yıldız, "Comparison of grey wolf, whale, water cycle, ant lion and sine-cosine algorithms for the optimization of a vehicle engine connecting rod," *Mater. Test.*, vol. 60, no. 3, pp. 311–315, Mar. 2018.

[43] S. Chamaani, S. A. Mirtaheri, and M. S. Abrishamian, "Improvement of time and frequency domain performance of antipodal vivaldi antenna using multi-objective particle swarm optimization," *IEEE Trans. Antennas Propag.*, vol. 59, no. 5, pp. 1738–1742, May 2011.

[44] H. J. Mohammed, J. M. Noras, R. A. Abd-Alhameed, Y. I. Abdulraheem, A. S. Abdullah, and R. S. Ali, "Design of a uniplanar printed triple band-rejected ultra-wideband antenna using particle swarm optimisation and the firefly algorithm," *IET Microw., Antennas Propag.*, vol. 10, no. 1, pp. 31–37, Jan. 2016.

[45] A.-K.-S. O. Hassan, A. S. Etman, and E. A. Soliman, "Optimization of a novel nano antenna with two radiation modes using Kriging surrogate models," *IEEE Photon. J.*, vol. 10, no. 4, pp. 1–17, Aug. 2018.

[46] B. Liu, H. Aliakbarian, S. Radiom, G. A. E. Vandenbosch, and G. Gielen, "Efficient multi-objective synthesis for microwave components based on computational intelligence techniques," in *Proc. 49th Annu. Design Autom. Conf. (DAC)*, San Francisco, CA, USA, 2012, pp. 3–7.

[47] S. Xiao, G. Q. Liu, K. L. Zhang, Y. Z. Jing, J. H. Duan, P. Di Barba, and J. K. Sykulski, "Multi-objective Pareto optimization of electromagnetic devices exploiting Kriging with Lipschitzian optimized expected improvement," *IEEE Trans. Magn.*, vol. 54, no. 3, pp. 1–4, Mar. 2018.

[48] G. Bramerdorfer and A.-C. Zavoianu, "Surrogate-based multi-objective optimization of electrical machine designs facilitating tolerance analysis," *IEEE Trans. Magn.*, vol. 53, no. 8, pp. 1–11, Aug. 2017.

[49] Z. Lv, L. Wang, Z. Han, J. Zhao, and W. Wang, "Surrogate-assisted particle swarm optimization algorithm with Pareto active learning for expensive multi-objective optimization," *IEEE/CAA J. Automatica Sinica*, vol. 6, no. 3, pp. 838–849, May 2019.

[50] J. Dong, W. Qin, and M. Wang, "Fast multi-objective optimization of multi-parameter antenna structures based on improved BPNN surrogate model," *IEEE Access*, vol. 7, pp. 77692–77701, 2019.

[51] Y.-S. Chen, "Application of multi-objective fractional factorial design for ultra-wideband antennas with uniform gain and high fidelity," *IET Microw., Antennas Propag.*, vol. 9, no. 15, pp. 1667–1672, Dec. 2015.

[52] D. I. L. de Villiers, I. Couckuyt, and T. Dhaene, "Multi-objective optimization of reflector antennas using Kriging and probability of improvement," in *Proc. IEEE Int. Symp. Antennas Propag. USNC/URSI Nat. Radio Sci. Meeting*, San Diego, CA, USA, Jul. 2017, pp. 985–986.

[53] J. A. Easum, J. Nagar, P. L. Werner, and D. H. Werner, "Efficient multiobjective antenna optimization with tolerance analysis through the use of surrogate models," *IEEE Trans. Antennas Propag.*, vol. 66, no. 12, pp. 6706–6715, Dec. 2018.

[54] S. Koziel and S. Ogurtsov, "Multi-objective design of antennas using variable-fidelity simulations and surrogate models," *IEEE Trans. Antennas Propag.*, vol. 61, no. 12, pp. 5931–5939, Dec. 2013.

[55] S. Koziel and A. T. Sigurðsson, "Multi-fidelity EM simulations and constrained surrogate modelling for low-cost multi-objective design optimisation of antennas," *IET Microw., Antennas Propag.*, vol. 12, no. 13, pp. 2025–2029, Oct. 2018.

[56] S. Koziel and A. Pietrenko-Dabrowska, "Rapid multi-objective optimization of antennas using nested Kriging surrogates and single-fidelity EM simulation models," *Eng. Comput.*, vol. 37, no. 4, pp. 1491–1512, Dec. 2019.

[57] S. Koziel and A. Pietrenko-Dabrowska, "Performance-based nested surrogate modeling of antenna input characteristics," *IEEE Trans. Antennas Propag.*, vol. 67, no. 5, pp. 2904–2912, May 2019.

[58] I. T. Jolliffe, *Principal Component Analysis*, 2nd ed. New York, NY, USA: Springer, 2002.

[59] K. Deb, *Multi-Objective Optimization Using Evolutionary Algorithms*. New York, NY, USA: Wiley, 2001.

[60] S. An, S. Yang, and O. A. Mohammed, "A Kriging-assisted light beam search method for multi-objective electromagnetic inverse problems," *IEEE Trans. Magn.*, vol. 54, no. 3, pp. 1–4, Mar. 2018.

[61] W. Lyu, F. Yang, C. Yan, D. Zhou, and X. Zeng, "Multi-objective Bayesian optimization for analog/RF circuit synthesis," in *Proc. 55th ACM/ESDA/IEEE Design Autom. Conf. (DAC)*, Jun. 2018, pp. 1–6.

[62] C. M. Fonseca, "Multiobjective genetic algorithms with application to control engineering problems," Ph.D. dissertation, Dept. Autom. Control Syst. Eng., University Sheffield, Sheffield, U.K., 1995.

[63] S. D. Unnsteinsson and S. Koziel, "Generalized Pareto ranking bisection for computationally feasible multiobjective antenna optimization," *Int. J. RF Microw. Comput.-Aided Eng.*, vol. 28, no. 8, Oct. 2018, Art. no. e21406.

[64] A. Amrit, L. Leifsson, and S. Koziel, "Multi-fidelity aerodynamic design trade-off exploration using point-by-point Pareto set identification," *Aerosp. Sci. Technol.*, vol. 79, pp. 399–412, Aug. 2018.

[65] S. Koziel, Q. S. Cheng, and J. W. Bandler, "Space mapping," *IEEE Microw. Mag.*, vol. 9, no. 6, pp. 105–122, Dec. 2008.

[66] N. M. Alexandrov and R. M. Lewis, "An overview of first-order model management for engineering optimization," *Optim. Eng.*, vol. 2, no. 4, pp. 413–430, Dec. 2001.

[67] A. Amrit, L. Leifsson, and S. Koziel, "Design strategies for multi-objective optimization of aerodynamic surfaces," *Eng. Comput.*, vol. 34, no. 5, pp. 1724–1753, Jul. 2017.

[68] A. Pietrenko-Dabrowska and S. Koziel, "Accelerated multiobjective design of miniaturized microwave components by means of nested Kriging surrogates," *Int. J. RF Microw. Comput.-Aided Eng.*, vol. 30, no. 4, Apr. 2020, Art. no. e22124.

[69] A. I. J. Forrester and A. J. Keane, "Recent advances in surrogate-based optimization," *Prog. Aerosp. Sci.*, vol. 45, nos. 1–3, pp. 50–79, Jan. 2009.

[70] B. Beachkofski and R. Grandhi, "Improved distributed hypercube sampling," in *Proc. 43rd AIAA/ASME/ASCE/AHS/ASC Struct., Structural Dyn., Mater. Conf.*, Apr. 2002, p. 1274.

[71] N. Kaneda, W. R. Deal, Y. Qian, R. Waterhouse, and T. Itoh, "A broadband planar quasi Yagi antenna," *IEEE Trans. Antennas Propag.*, vol. 50, pp. 1158–1160, 2002.

[72] M. G. N. Alsath and M. Kanagasabai, "Compact UWB monopole antenna for automotive communications," *IEEE Trans. Antennas Propag.*, vol. 63, no. 9, pp. 4204–4208, Sep. 2015.

SLAWOMIR KOZIEL (Senior Member, IEEE) received the M.Sc. and Ph.D. degrees in electronic engineering from the Gdansk University of Technology, Poland, in 1995 and 2000, respectively, the M.Sc. degrees in theoretical physics and in mathematics, in 2000 and 2002, respectively, and the Ph.D. degree in mathematics from the University of Gdansk, Poland, in 2003. He is currently a Professor with the Department of Engineering, Reykjavik University, Iceland. His research interests include CAD and modeling of microwave and antenna structures, simulation-driven design, surrogate-based optimization, space mapping, circuit theory, analog signal processing, evolutionary computation, and numerical analysis.

ANNA PIETRENKO-DABROWSKA (Senior Member, IEEE) received the M.Sc. and Ph.D. degrees in electronic engineering from the Gdansk University of Technology, Poland, in 1998 and 2007, respectively. She is currently an Associate Professor with the Gdansk University of Technology, Poland. Her research interests include simulation-driven design, design optimization, control theory, modeling of microwave and antenna structures, and numerical analysis.